Thermal design methodology of hot and chill plates for photolithography

D.P. DeWitt
School of Mechanical Engineering
Purdue University
West Lafayette, IN 47907

T.C. Niemoeller
Technometrics, Inc.
West Lafayette, IN 47906

Chris A. Mack
FINLE Technologies, Inc.
Austin, TX 78716

Gil Yetter
SEMATECH, Inc.
Austin, TX 78741

Abstract

The major requirement for hot- and chill-plate designs is that they provide repeatable and uniform process conditions thereby assuring consistent photoresist quality. A collection of feature-based thermal models has been developed to predict temperature-time histories considering plate construction features including chuck heating/cooling methods, sensor placement with a PID control algorithm, and effects due to vacuum grooves, access holes, support pins and edge-gap. These models can be used by designers and process technologists to assess new approaches, optimize current design and set performance specifications.

1. Introduction

Hot-plate prebaking of conventional positive photoresist is intended to drive off solvent used for spin coating the resist, thereby densifying and stabilizing the film. A chill plate is also used after the hot plate to add control to the process and to increase throughput. The proper control of photoresist prebaking is extremely important for two reasons: resist thickness control and control of the chemical changes upon baking which influence the development properties of the resist and the resulting critical dimensions. The major requirements for hot and chill plate designs are that they provide repeatable and uniform process conditions thereby assuring consistent quality.

To illustrate the effects of plate construction features on thermal performance and its effect on photoresist characteristics, a collection of feature-based heat and mass transfer models have been developed which can be used by designers to assess new approaches, optimize current designs, and set performance specifications. These heat transfer models will be described and their application to typical process conditions will be illustrated. The mass transfer models are described in a companion paper[1].

0-8194-1491-3/94/$6.00

Two sets of heat transfer models are developed which provide the temperature-time history of a wafer, initially at a uniform temperature, which is suddenly thermally coupled to the chuck. The models include these features: wafer-chuck interface contact- or gap proximity-thermal resistance, convection cooling on the wafer top surface, as well as different methods for maintaining the chuck lower surface temperature. The *first* set is one-dimensional, transient models providing wafer surface time-to-heat (or -chill) as a function of wafer-chuck physical dimensions, thermal properties and thermal conditions. One of these models simulates the wafer-chuck system being heated by proportional-integral-derivative (PID) control action. The *second* set is two-dimensional heat transfer models that provide for estimating the temperature non-uniformity effects caused by construction features including vacuum grooves, instrumentation access holes, proximity heating support pins, and edge effects with proximity heating. One experiment was conducted to generate data on plate performance. The temperature-time history of a silicon wafer was observed for a typical hot plate and provided information useful for comparison with the one-dimensional, transient heat transfer models.

2. Thermal Models of the Plates

For these models, the system is composed of the *wafer,* initially at a uniform temperature, which is suddenly thermally coupled to the *chuck.* The elements common to these models, summarized in Table 1, include the wafer and chuck subjected to these thermal processes:

- Convection on the *upper surface* of the wafer,
- Thermal resistance due to conduction (contact) and to convection and/or radiative exchange (proximity) processes in the *interfacial or gap region* between the wafer and the chuck, and
- Convection and/or applied heat flux at the *lower surface* of the chuck.

The thermophysical properties required for the chuck and wafer materials include the density, specific heat and thermal conductivity. Geometrical parameters of the system include wafer and chuck thicknesses and, if appropriate, dimensions of such features as a groove, access hole and gap.

The software platform for the models is TK Solver (Version 2), a high level equation-solver complete with graphics and library features [2]. A menuing system for all the models of this report, referred to as LITHOPLT, permits the user to launch individual models from the TK platform. The analyses for all of the models are based upon a finite-difference numerical method (center-difference with temperature and solvent concentration *and* forward-difference or implicit with time discretization) [3].

2.1 Wafer Temperature-Time History

These models are based upon a *one*-dimensional, transient heat transfer analysis of the wafer-chuck system illustrated in Figure 1(a). The wafer (w), of thickness, L_w, at a uniform temperature, $T_w(x,0)$, is suddenly thermally coupled to the chuck (c), also at a uniform but different temperature, $T_c(x,0)$, and of thickness, L_c. In the interfacial region (or gap) between the wafer and chuck, the thermal resistance can be treated as due to

- A thermal contact resistance, R_{tc}", if the wafer *contacts* the chuck directly, or

- The combined processes of convection (coefficient, h_{wc}) and radiation exchange (with wafer and chuck emissivities, ε_w and ε_c) if a gap of separation distance, L_g, is present for *proximity* heating/cooling.

The upper surface of the wafer experiences a convection process with the ambient air at a temperature, T_∞, and convection coefficient, h_w.

The lower surface of the chuck, can be subjected to three different sets of conditions. Figures 1(b) and (c) illustrate, respectively, a convection process with specified fluid temperature and a convection coefficient (T,h) or an applied heat flux (q_s"). For each of these conditions, it is possible to specify constant or pre-programmed values (any user-specified function) for the process variables during a number of *wafer-on* and -*off* conditions.

Figure 1(d) illustrates the model wherein the heat flux to the lower surface of the chuck is controlled by a proportional-integral-derivative (PID) algorithm. This standard algorithm provides control action determined by three parameters,

- K_p, proportional sensitivity or gain,
- T_i, integral time, and
- T_d, derivative time.

The actuating temperature error is determined from the difference between the set point temperature, T_{set}, and the temperature at the control position, T_{con}, which can be any user-selected location within the chuck. The cycle time is defined by the user in terms of *wafer-on* and *wafer-off* time intervals. The model can be run for a prescribed number of cycles selected by the user.

2.2 Wafer Temperature Non-Uniformity

These models are based upon a *two*-dimensional, transient heat transfer analysis of the wafer-chuck system illustrated in Figure 2(a). As with the prior models, the wafer (w), of thickness L_w, at a uniform temperature, $T_w(x,0)$, is suddenly thermally coupled to the chuck (c), also at a uniform but different temperature, $T_c(x,0)$, and of thickness, L_c. In the interfacial region (or gap) between the wafer and chuck, the thermal resistance can be prescribed by an arbitrary function. This feature allows for examining what influence variable contact or proximity thermal resistance can have on the wafer surface temperature distribution.

The upper surface of the chuck experiences a convection process with a fluid at temperature, T_∞ , and a convection coefficient that can be prescribed by an arbitrary function thereby representing conditions appropriate for the flow field above the wafer. The lower surface of the chuck can experience either a convection process (T_∞,h) or an applied heat flux (q_s"), both of which can be specified by arbitrary functions. For the latter boundary condition, it is possible to simulate the presence of discrete spacing between elements of a heating coil. The lateral (or medial) edge of the wafer-chuck system can be specified by convection processes with a fluid at uniform prescribed temperature and convection coefficients.

Four models, representing special plate features, are illustrated in Figures 2(b-e). These models provide the temperature distribution on the wafer surface, as a function of time after being placed on the plate, in the vicinity of the feature:

- Vacuum groove, of depth d and width 2w,
- Access hole, with shoulder and flat bottom, for instrumentation sensor,
- Support pin for use in proximity heating/cooling, and
- Wafer-chuck gap at the lateral edge.

Several plotting options are available for each of the models representing temperature differences (non-uniformity) across the wafer surface, temperature-time history of specific locations, and, in some instances, heat flux distributions for various processes at boundaries.

3. Applications of the Plate Heat Transfer Models

To illustrate the nature of the analyses possible by these models, five applications are presented here.

3.1 Hot Plate Time-To-Heat

The temperature-time history for a wafer, initially at 23 °C, which is contact or proximity heated by a 100 °C chuck, is shown in Figure 3 for different thermal conditions. The solid and dashed lines correspond, respectively, to chucks (20 mm thickness) fabricated from aluminum alloy and pure copper. While the thermal diffusivity of pure copper is nearly 60% greater than that of the aluminum alloy, its effect for proximity heating with a gap of 0.2 mm (0.008 in) is negligible. However, for good vacuum contact heating, the decrease in time-to-heat could be significant.

The experimental observations for a laboratory-grade, aluminum-alloy vacuum chuck are show by the symbols (♦) [4]. It is apparent by comparison with the model curve (solid line), that the thermal contact resistance must be less than 0.00035 $m^2 \cdot K/W$, a value arbitrarily chosen to represent typical base conditions.

From this comparison of the model results for contact- and proximity-heating conditions and of the experimental observations, that the nature of the thermal coupling at the wafer-chuck interface is the controlling effect on the time-to-heat. Further understanding of the thermal performance could be gained by examining the effects due to other parameters such as the convection coefficient at the wafer surface and thickness of the chuck. Particularly interesting is to examine the temperature-time history of the chuck near the wafer interface as a means to better understand how improvements might be possible with respect to controlling imbedded heaters.

3.2 Chill Plate Feasibility Study

A recent paper [5] reported on an experimental study to determine if chilling by proximity could be done in a reasonable time. Such a feasibility study could be performed using an appropriate one-dimensional, transient model (ABC-1), the results of which are shown in Figure 4. Note first the broken curve representing the time-temperature history for a wafer, originally at 100 °C, cooling in quiescent air; that is, not in contact with

the chill plate. From the experimental study, as well as the model results not shown, it takes nearly 250 seconds for the wafer to reach 20 °C.

The time-to-cool curves for proximity chilling with gap spacing of 0.318 and 0.635 mm (0.0125 and 0.025 in) are shown when the chill plates are maintained at 12 and 16 °C, respectively, represented by solid and dashed lines. From these curves, it can be seen that the wafer can be chilled from 100 °C to 30 °C in less than 50 seconds with a chill plate at 12 °C, for the larger proximity gap. Similarly, the wafer can be chilled to 20 °C in less than 80 seconds with a chill plate at 16 °C. These model predictions are identical to the observations drawn from the experimental study. The good agreement creates confidence in the modeling and provides the opportunity to explore other techniques. For example, a technique for cooling a wafer to 20 °C, without an undershoot, in less than 30 seconds, could be demonstrated.

3.3 PID Control Algorithm

For the proportional-integral-differential (PID) control arrangement shown in Figure 1(d), a one-dimensional, transient model was used to simulate a series of wafers heated by a hot plate. The PID control over the heating on the bottom of the chuck is in the form

$$P(t) = K_p e(t) + K_p T_d \frac{de(t)}{dt} + \frac{K_p}{T_i}\int_0^t e(t)dt$$

where in the example $K_p = 600\ \left(W/m^2\right)/°C$, $T_d = 0.1$ s and $T_i = 200$ s. The value of e(t) is the difference between the set point, 100 °C, and the temperature of the sensor in the chuck. An additional 1000 W/m^2 is added 8 s before the wafer is placed and removed 5 s after placement. The wafers, initially at 20 °C, are placed on the chuck every 40 s and removed after a 30 s bake.

Figure 5 illustrates the results of the simulation for 3 cycles. Figure 5(a,b) shows the temperature-time history for the wafer (solid line), the upper surface of the chuck (dashed line) and the lower surface of the chuck (dot-dash line). Figure 5(c) shows the heater input as a function of time. The wafers are not experiencing the same thermal history from cycle-to-cycle, indicating that the control settings are not optimal. We could re-run the model with different control parameters until repeatable cyclic heating has been obtained. By so doing, we will develop an understanding of their influence on wafer temperature-time history.

3.4 Temperature Non-Uniformity Above a Vacuum Groove

For the vacuum groove arrangement shown in Figure 2(b), the two-dimensional, transient model was used to predict the temperature nonuniformity caused by the variation in thermal coupling between the wafer and the chuck. Figure 6 shows the temperature depression, measured as the difference between the wafer surface temperature far removed from the groove and the temperature above the groove, as a function of time for the first five seconds following heating contact. Results for longer elapsed times show that the steady-state depression is nearly zero.

From Figure 6, curve (1) represents contact heating with a very high thermal resistance illustrating that, under these limiting conditions, the effect of the groove is minimal, but there is an offset that eventually vanishes.

Curve (2) represents a more typical application situation with low thermal contact resistance and a vacuum groove of 1.42 mm width and 0.71 m depth (0.056 by 0.028 in) showing that, at early times, the temperature depression amounts to more than 1 °C. If the groove width is doubled, curve 3, the maximum temperature depression increases to more than 2.5 °C.

Do wafer temperature non-uniformities such as those demonstrated by curve (2) and (3) have any appreciable effect on photoresist? Anecdotal experiences suggest that vacuum grooves, under some conditions, can create thermal anomalies that show up in variable photoresist characteristics. As will be pointed out in our companion paper [1], the models provide the means to explore temperature effects on photoresist. The benefit to such a study would be in gaining an understanding of how, and to what extent, hot plate construction features influence photoresist characteristics.

3.5 Effect of Discrete Heater Spacing

Figure 7 shows the steady-state temperature distribution across four surfaces of the wafer-chuck system with 5-mm wide heaters on 20-mm spacing applied to a 25-mm thick aluminum alloy chuck. A vacuum groove of 5-mm width and 2.5-mm depth is also included as a feature in this simulation. The waviness of the temperature distribution across the chuck lower surface shows peaks at the centers of the discrete heaters. Along the chuck upper surface, the temperature distribution is nearly uniform, but doesn't exhibit any waviness. Likewise the temperatures across the wafer lower and upper surfaces show no waviness, but do show the temperature depression caused by the presence of the vacuum groove.

4. Usefulness of the Models

The goal of plate design is to create a tool that allows for consistent wafer-photoresist characteristics. Having an understanding of how plate features influence temperature-time histories and temperature non-uniformities is only one part of the design process, but it is the initial and most important part.

4.1 Applications: Design and Evaluation

The models are valuable for design activities, especially to establish the feasibility of new approaches and for process performance evaluation. The chill plate study above could be extended to establish whether a practical plate cooling scheme could be identified to chill the wafer to 20 °C, with no undershoot, in less than 30 seconds. One of the models could be used to determine what effect control sensor location within the chuck has on a PID-controlled heating system. In what manner does the spacing of discrete heater elements influence temperature uniformity of the wafer? Or the variability of the convection coefficient above the wafer surface?

As confidence is gained in using these feature-based models, first in simple applications, it will be possible to extend the analyses to include higher-order effects. While a keen intuition is essential for good

design, modeling provides the means to quantify effects, thereby developing a broader, more dependable knowledge base.

4.2 Recommendations for Future Work

The work performed here provides a sound theoretical basis for an understanding of heat and mass transfer effects in hot and chill plate baking of photoresist and a preliminary set of tools to quantify these effects. Future work in this area falls into three categories: 1) further model development including airflow effects on the resulting convection coefficients; 2) application of the heat transfer models to hot and chill plate design and analysis; and 3) coupling of the heat and mass transfer models of the photoresist to subsequent models to predict their impact on final resist linewidth. The final category would include the use of the heat and mass transfer models in the modeling of chemically amplified resists.

4.3 Using and Obtaining the Models

The menuing system for the models of this study is called LITHOPLT and permits the user to launch individual models from TK Solver (Version 2) installed on any IBM-compatible machine. A product of Universal Technical Services, Inc. [2], TK is a high level equation-solver software package that *solves* the model for the prescribed input variables and provides output results in tabular and graphical formats. By changing values of the input variables, the user can explore effects on plate temperature distributions or film characteristics.

TK Solver is an easy language to learn and only a modest understanding is required to run the models. Two software packages of general-purpose heat transfer models, entitled HEAT and *Exploring Heat Transfer with TK Solver*, are available from UTS. HEAT contains 143 models for common physical systems experiencing processes of conduction, convection and radiation including an extensive library of thermophysical properties of selected materials and fluids. Prepared for the academic market, *Exploring* is an abbreviated version with 43 models and includes a manual containing a tutorial and several example problems and their models. The models of these packages, as well as those of LITHOPLT, are based upon nomenclature and equations in a widely used text [3].

Further details on the models and a copy of LITHOPLT (one 1.44 Mb diskette) are available to SEMATECH and SEMI/SEMATECH members [6]. This report includes extensive appendices with detailed descriptions of the models, icons to illustrate the plate/film thermal conditions, TK Solver Variable Sheets introducing the system parameters, and typical results. The appendices serve as a user's manual for the use of the models.

References

1. C.A. Mack, D.P. DeWitt, B.K. Tsai, and G. Yetter, "Modeling Solvent Evaporation Effects for Hot Plate Baking of Photoresists," SPIE Paper 2195-51, March 1994

2. *TK Solver*, Universal Technical Systems (UTS), 1220 Rock St., Rockford IL 61101. See also the software application packages *Exploring Heat Transfer with TK Solver* and *HEAT*.

3. F.P. Incropera and D.P. DeWitt, *Fundamentals of Heat and Mass Transfer*, 3rd Ed., Section 5.9, John Wiley & Sons, New York, 1990.

4. G. Yetter, "Wafer Heat Ramp Measurements," Interoffice Memorandum, Department 820, SEMATECH, October 7, 1993.

5. B. Mohondro, P. Gaboury, J. Clayton, and D. Dumpert, "Characterizing and Understanding Thermal Anomalies in Photoresist Processing Tools Utilizing IR Imaging Technology," *Proceedings of the OCG Microlithography Seminar, Interface '93,* OCG Microelectronic Materials, Inc., (September 1993) pp. 101-118.

6. G. Yetter (SEMATECH coordinating author), D.P. DeWitt, T.C. Niemoeller and C.A. Mack, "Hot Plate Heat and Mass Transfer Modeling," SEMATECH, Document No. 93122137A-TR, March 1994.

Table 1: Summary of the Models

Wafer Suddenly Thermally Coupled to the Chuck

Temperature-Time History of Wafer

One-Dimensional, Transient Heat Transfer

Designation	Chuck Lower Surface Boundary Condition
ABC-1	Constant convection process (T_∞, h)
-2	Programmed convection process; $T_\infty(t)$ and h
-3	Constant heat flux, q_s''
-4	Programmed heat flux, $q_s''(t)$
-5	PID controlled heat flux for set point temperature, T_{set}
-6	Test code to determine PID algorithm coefficients

Temperature Nonuniformity Across Wafer Surface

Two-Dimensional, Transient Heat Transfer

Designation	Special Chuck Feature
CT	Vacuum groove
DT	Instrument access hole
ET	Proximity support pin
FT	Proximity gap at wafer edge

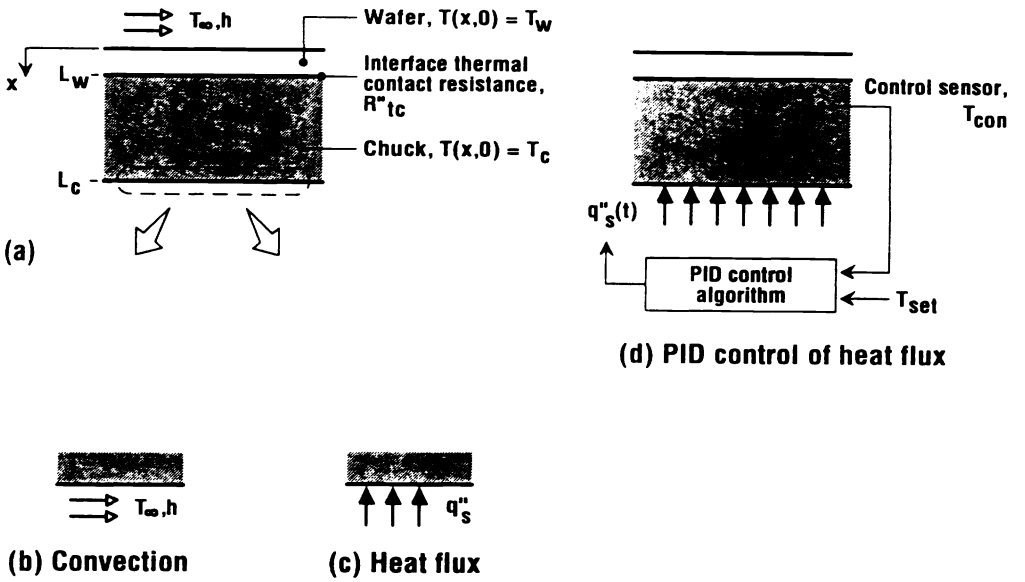

Figure 1. One-dimensional, transient heat transfer models for predicting wafer time-to-heat (or -chill): (a) wafer at initial temperature T_w suddenly coupled to a chuck at initial, uniform temperature T_c with convection on the wafer surface, interface thermal contact/proximity resistance, and with lower chuck surface subjected to (b) convection process, (c) applied heat flux, and (d) PID control of heat flux with sensor T_{con}.

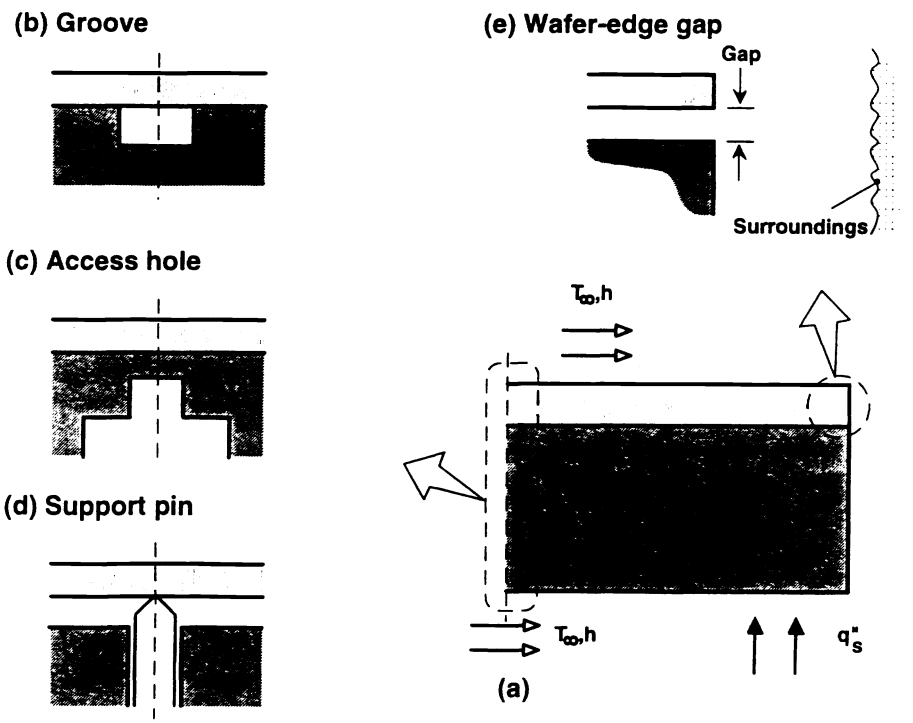

Figure 2. Two-dimensional, transient heat transfer models for predicting (a) wafer surface temperature nonuniformity with time due to the effects of (b) vacuum groove, (c) instrument access hole, (d) proximity support pin, and (e) proximity gap at the wafer-chuck edge.

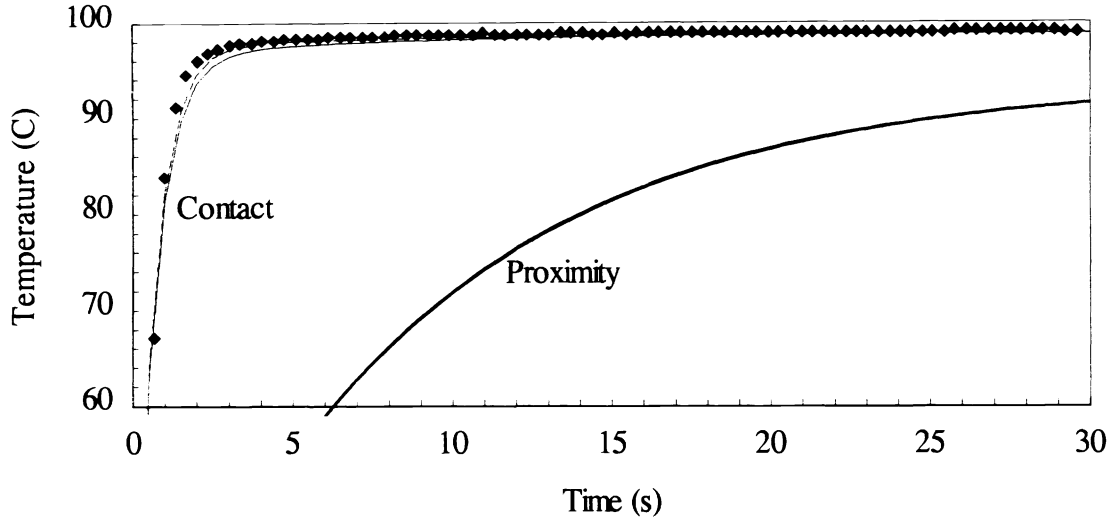

Figure 3. The influence of interface thermal contact resistance on the temperature-time history for a wafer, initially at 23 °C, which is contact or proximity heated by an aluminum alloy (solid line, k=175 W/m·K) or pure copper (dashed line, k=400 W/m·K) chuck at 100 °C. The contact thermal resistance is 0.00035 m^2·K/W, typical for good vacuum hold-down conditions, and the proximity gap spacing is 0.2 mm (0.008"). Symbols (♦) represent experimental observations for an aluminum alloy chuck.

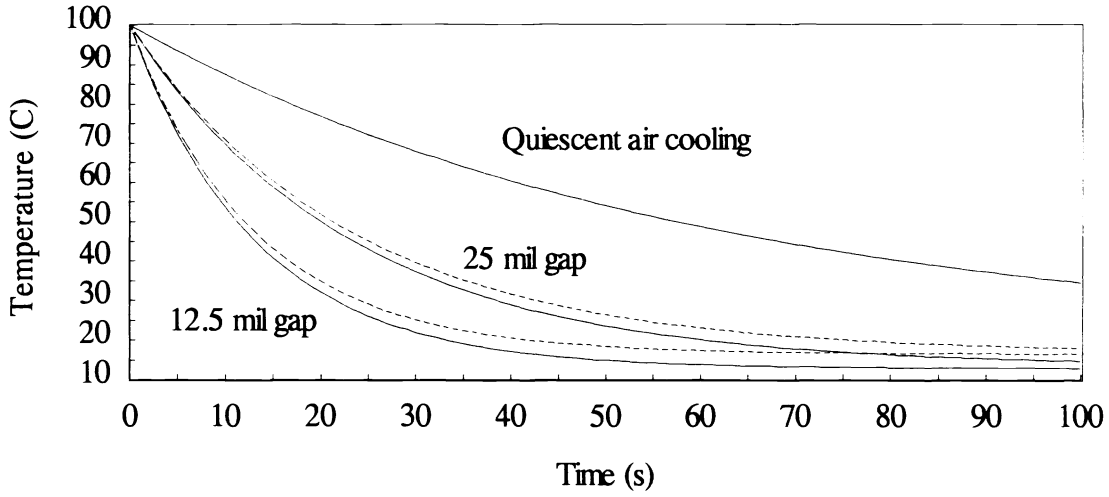

Figure 4. Application study to determine the feasibility of proximity cooling a wafer from 100 °C to 30 °C in less than 50 seconds or to 20 °C in less than 80 seconds, with chill-plate temperatures at 12 °C and 16 °C, solid and dashed lines, respectively, for two values of the proximity gap spacing, 0.318 and 0.635 mm (0.0125 and .025 in), respectively. Also shown is the temperature-time history for a wafer cooling in quiescent air.

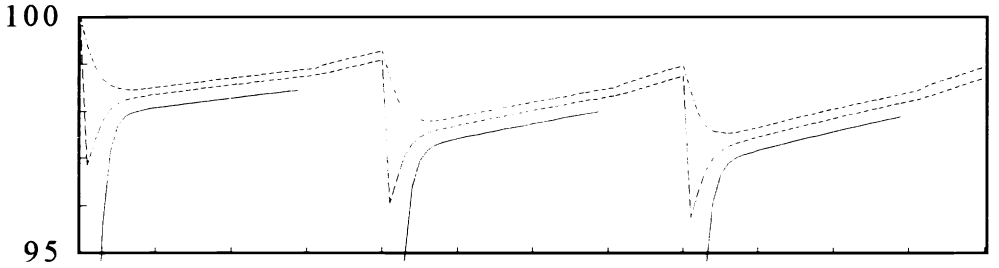

(a) Temperature history

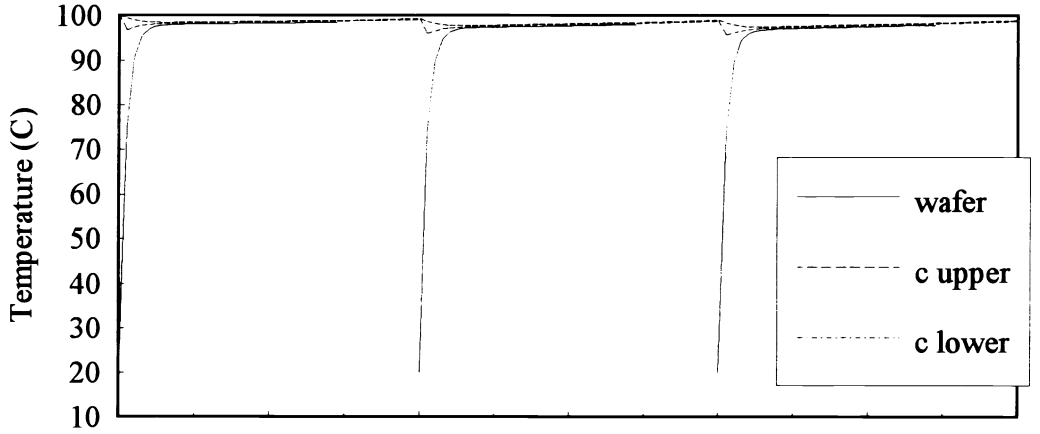

(b) Temperature history

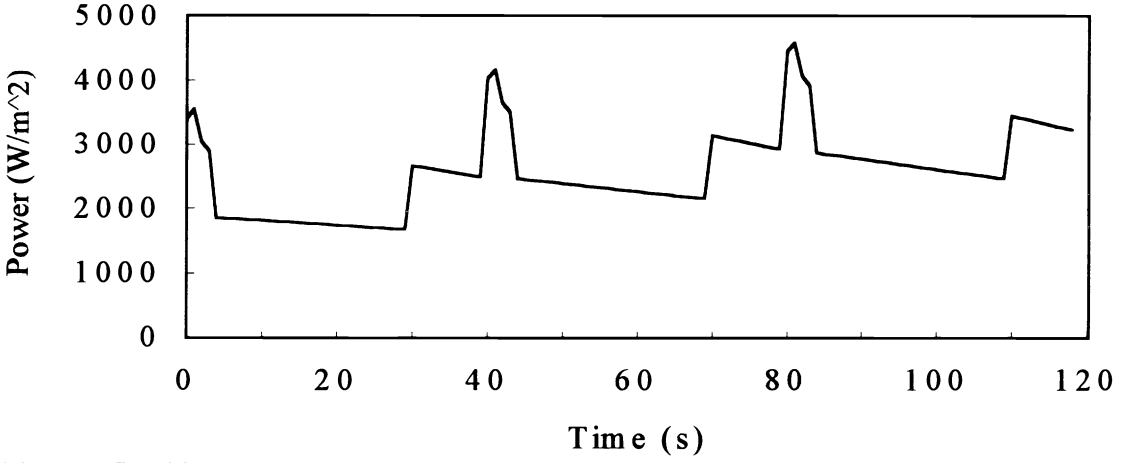

(c) Heat flux history

Figure 5. Processing a series of 3 wafers: (a,b) Temperature history for the chuck lower (upper), chuck upper (middle) and wafer upper surfaces (lower) and (c) output of heater.

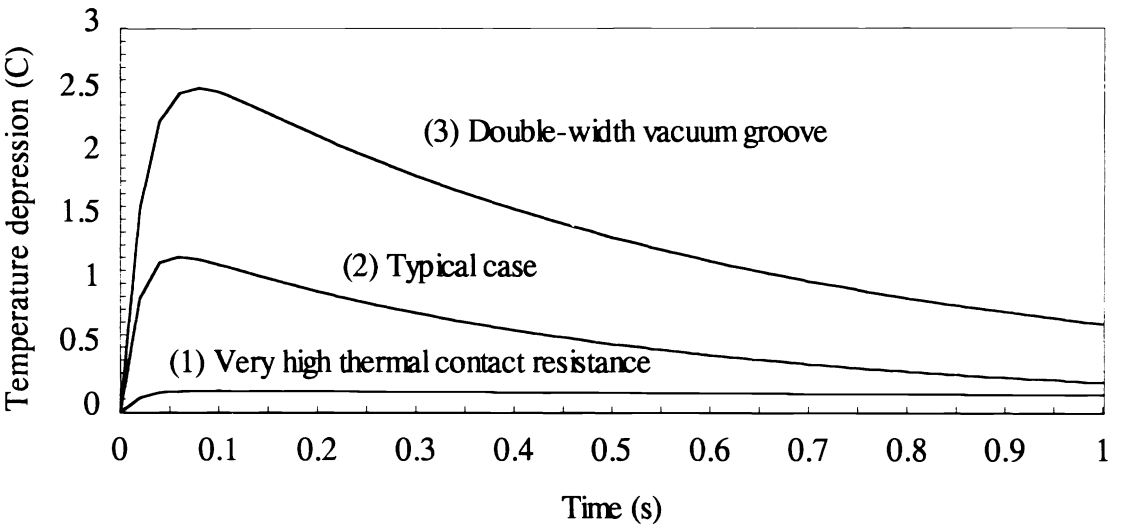

Figure 6. Depression in wafer surface temperature directly above the vacuum groove of 1.42 mm width and 0.71 mm deep (0.056 by 0.028 in) as a function of time with (1) very high (0.003 m^2 K/W) and (2) typical low (0.00035 m^2 K/W) thermal contact resistances. The effect of doubling the width of the vacuum groove for the lower contact resistance condition is shown as curve 3.

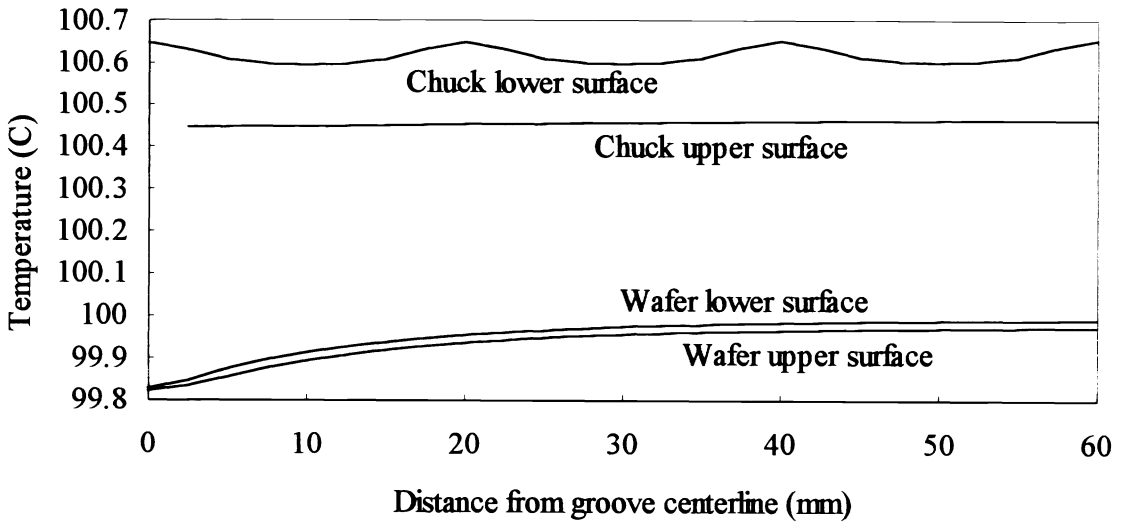

Figure 7. Effect of discrete heater spacing on temperature distribution in wafer and chuck. Heaters are 5 mm wide, spaced 20 mm apart.

Appendix
Method of Solution for the Models

The method of solution and key relations for the heat transfer models will be briefly summarized.

The One-Dimensional Transient Models

The heat diffusion equation (HDE) in differential form

$$\frac{\partial}{\partial x}\left(\frac{\partial T}{\partial x}\right)=\frac{\rho c}{k}\frac{\partial T}{\partial t} \tag{A-1}$$

expresses the conservation of energy requirement and must be written for the wafer (w) and chuck (c) regions in the x-coordinate space. For the HDE in each region, one initial and two boundary conditions must be specified to obtain the temperature distribution. The initial conditions are prescribed as uniform throughout each region, $T_w(x,0)=T_{w,i}$ and $T_c(x,0)=T_{c,i}$ respectively. The boundary conditions are:

- upper wafer surface: convection process with a fluid
- lower chuck surface: convection with a fluid or applied heat flux
- interface between the wafer and chuck: thermal resistance due to processes of conduction, convection or radiation exchange.

The last situation specifies two conditions, placing requirements on the temperature distribution (continuous, only if no thermal resistance is present) and on the heat flux (equal in both regions) across the interface.

The HDEs for the wafer and chuck regions are coupled through the interface boundary conditions making the analytical solution very complicated. A numerical method of solution for the wafer-chuck system is readily formulated and easily solved following procedures described in many heat transfer texts[2]. In finite-difference form, the discretized HDE for each region has the form

$$(1+2\mathrm{Fo})T_m^{p+1}-\mathrm{Fo}\left(T_{m-1}^{p+1}+T_{m+1}^{p+1}\right)=T_{m,n}^{p} \tag{A-2}$$

where Fo is the Fourier number,

$$\mathrm{Fo}=\frac{\alpha\Delta t}{(\Delta x)^2} \tag{A-3}$$

and is the thermal diffusivity,

$$\alpha=\frac{k}{\rho c} \tag{A-4}$$

The indices (m,p) identify the space and time discretized coordinates so that $x = m \cdot \Delta x$ and $t = p \cdot \Delta t$. The choices of the nodal spacing, Δx, and time increment, Δt, influence the precision of the solution as well as the computational time to solve for the temperature distribution, T(m,p). The form of the FDE, Equation A-2, is based upon a central-difference approximation for the spatial derivatives and a backward-difference approximation to the time derivative. This is referred to also as the implicit method of solution.

The FDEs for the boundary nodes are obtained by writing an energy balance on a suitably defined control volume about the node. The FDEs for the upper wafer and lower chuck surfaces follow classical treatment and are shown in Table A-1. For the wafer-chuck interface, it is useful for reasons to be explained later to introduce an interface *region* represented by a single node designated as T_{if} in Figure A-1. The region is prescribed by the thermal properties density, ρ_{if}, specific heat, c_{if}, and spatial increment, Δx_{if}, chosen such that its thermal capacitance, $(\rho c \Delta x)_{if}$, is negligible compared to neighboring nodes in the wafer and chuck regions. The processes associated with the interface are expressed as a thermal resistance, R''_{tc}, the form of which is determined by the appropriate rate equation,

Conduction:

$$R''_{cond} = \frac{\Delta x_g}{k_g} \tag{A-5}$$

where Δx_g is the wafer-chuck gap and k_g is the thermal conductivity of the fluid in the gap;

Convection:

$$R''_{conv} = \frac{1}{h_g} \tag{A-6}$$

where h_g is the convection coefficient within the gap region; and

Radiation exchange:

$$R''_{rad} = \frac{1}{h_{rad}} \tag{A-7}$$

$$h_{rad} = \frac{\sigma\left(T_{w,s} + T_{c,s}\right)\left(T_{w,s}^2 + T_{c,s}^2\right)}{1/\varepsilon_w + 1/\varepsilon_c - 1} \tag{A-8}$$

where ε_w and ε_c are the emissivities of the wafer and chuck surfaces (assumed infinite parallel planes) and σ is the Stefan-Boltzmann constant, $5.67 \times 10^{-8}\ W/m^2 \cdot K$. Note that the radiation exchange process has been linearized and that the radiation coefficient h_{rad} is a function of the wafer and chuck surface temperatures.

The FDEs for the nodes on the wafer lower surface, the interface, and the upper chuck surface are obtained by performing energy balances on the respective nodes as represented in Figure A-1. The results are:

Wafer lower surface (w, m=s)

$$\left[1+2\mathrm{Fo}\left(1+2\mathrm{Bi}_r\right)\right]T_m^{p+1}-2\mathrm{Fo}\left(T_{m-1}^{p+1}+2\mathrm{Bi}_r T_{if}^{p+1}\right)=T_m^p \tag{A-9}$$

Interface node (if)

$$\left(1+4\mathrm{Bi}_r\mathrm{Fo}\right)T_{if}^{p+1}-2\mathrm{Bi}_r\mathrm{Fo}\left(T_{w,s}^{p+1}+T_{c,s}^{p+1}\right)=T_{if}^p \tag{A-10}$$

Chuck upper surface (c, m=s)

$$\left[1+2\mathrm{Fo}\left(1+2\mathrm{Bi}_r\right)\right]T_m^{p+1}-2\mathrm{Fo}\left(T_{m+1}^{p+1}+2\mathrm{Bi}_r T_{if}^{p+1}\right)=T_m^p \tag{A-11}$$

where the Biot number, based upon the thermal resistance, is

$$\mathrm{Bi}_r=\frac{\Delta x}{k\cdot R_t''} \tag{A-12}$$

The initial conditions (p=0) for the wafer and chuck regions are prescribed by setting the interior and boundary nodal temperatures to either $T_{w,i}$ or $T_{c,i}$. The initial condition for the interface region (a single node) can be chosen as the average between the wafer and chuck initial temperatures, $T_{if,i}=(T_{w,i}+T_{c,i})/2$. If the thermal inertia (product of thermal conductivity, density and specific heat, $k\rho c$) for the two regions is appreciably different, it is more appropriate to use the form

$$T_{if,i}=\frac{(k\rho c)_w^{1/2}T_{w,s}+(k\rho c)_c^{1/2}T_{c,s}}{(k\rho c)_w^{1/2}+(k\rho c)_c^{1/2}} \tag{A-13}$$

By utilizing a low thermal capacitance interface region (node) and setting its initial temperature at a value consistent with an energy balance across the interface, we are assured of a stable, non-oscillatory solution at early times. This approach also makes the solution method robust such that reliable results are obtained with a wide range of thermal resistance magnitudes from nearly zero (perfect contact) to very large (adiabatic condition).

Two-Dimensional, Transient Models

Extending the heat transfer analysis to two dimensions -- either cartesian or cylindrical-axisymmetric coordinates -- requires tedious work to derive the appropriate forms of the finite-difference forms of the

nodal energy equations. As can be seen from Figure 2, it is necessary to derive FDEs for several different types of corners and edges. These derivations are straightforward but require considerable attention to detail. The resulting FDEs will be similar in appearance, for example to Equation A-2, except for the presence of two additional nodal temperatures representing the second coordinate direction.

Method of Solution

The resulting FDEs, each representing an energy balance about a node whose temperature is unknown, form a set of algebraic equations that need to be solved simultaneously. For each time step the temperature distribution is obtained, T(m,p) if one-dimensional and T(m,n,p) if two-dimensional. If the analysis is one-dimensional, a matrix-inversion method of solution can be used. Two-dimensional systems of equations are solved iteratively. If the radiation exchange process of Equation A-8 is represented, it is necessary that the linearized form of the rate equation be employed. Since h_{rad} is a function of the wafer and chuck surface temperatures, the best procedure is to update its value after each time-step calculation. The TK Solver engine uses the Newton-Raphson method to generate progressively better guesses for the temperatures; the precision of the results is user-specified.

Table A-1
Finite-difference equations for selected wafer and chuck boundary nodes

Upper wafer surface, convection process:

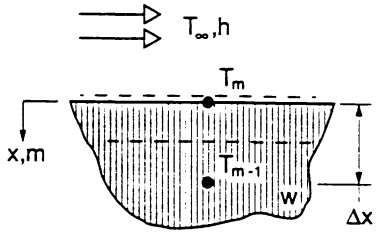

$$(1+2\mathrm{FoBi})T_m^{p+1} - 2\mathrm{Fo}T_{m+1}^{p+1} = T_m^p + 2\mathrm{BiFo}T_\infty$$

Lower chuck surface, applied heat flux:

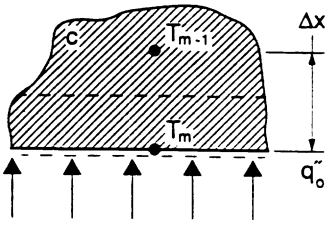

$$(1+\mathrm{Fo})T_m^{p+1} - 2\mathrm{Foq}_o''\Delta x / k = T_m^p$$

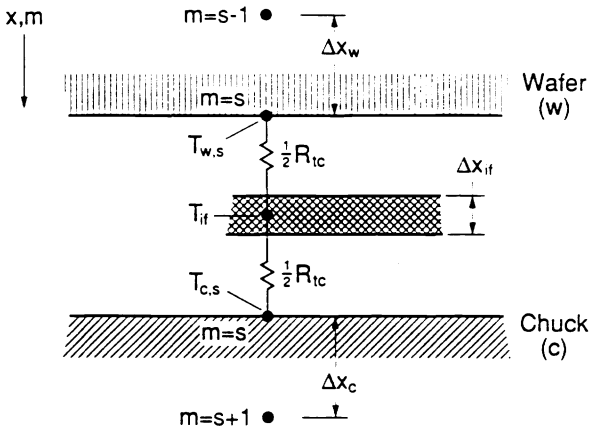

Figure A-1. Nodal arrangement in the vicinity of the interface region between the wafer and the chuck.